EurJOC
European Journal of Organic Chemistry

Research Article
doi.org/10.1002/ejoc.202101272

Chemistry Europe
European Chemical Societies Publishing

www.eurjoc.org

Special Collection

Primary Amine Catalyzed Activation of Carbonyl Compounds: A Study on Reaction Pathways and Reactive Intermediates by Mass Spectrometry

Antonia Iazzetti,[a] Giulia Mazzoccanti,[b] Giorgio Bencivenni,[c] Paolo Righi,[c] Andrea Calcaterra,[b] Claudio Villani,[b] and Alessia Ciogli*[b]

The field of organocatalysis is expanding at a fast pace. Its growth is sustained by major stimuli, such as the effort toward an understanding of the mechanisms of reaction and catalytic processes in general, the elucidation of basic properties leading to stereocontrol and the search for broad applicability and scalability of the synthetic methodology. This paper reports a thorough study based on ESI-MS spectrometry of amino-organocatalyzed model reactions under different experimental conditions. Off-line reaction monitoring of mixtures containing different catalytic systems, by ESI-MS^n showed the presence of several putative intermediate species, either in their protonated or sodiated forms. In addition, enantioselective chromatography of crude reactions provides the stereochemical outcome of asymmetric reactions. The bulk of the data collected offers a clue of the intricate pathways occurring in solution for the studied reactions.

Introduction

Asymmetric aminocatalysis represents today the most widely used organocatalytic technique to functionalize, with high stereocontrol, carbonyl compounds in α-position as well, for the unsaturated ones, in γ- and ε-positions.[1] No doubt, the primary amines entered the catalysis field slowly but, in the last 10–15 years, have been reinvestigated and established as effective organocatalysts in asymmetric aldol, Michael, Mannich, Diels-Alder, aminations, 1,3-dipolar cycloadditions, and domino reactions.[2] As for the secondary, primary amines act mostly in acid conditions through the iminium and enamine intermediates[3] and the stereocontrol of product depends also on the nature of acid cocatalyst, not necessarily chiral.[4] Indeed, the chiral induction to the reaction product, beyond of mere formation of covalent bonds, is mainly dictated by electronic (e.g., hydrogen bonding and π–π stacking) and steric interactions between active intermediates (iminium ion or enamine), Michael acceptor and acid co-catalyst to build the perfect catalytic cycle. In other words, weak and non-covalent interactionsare the driving force accountable for the assembly of catalytic partners and reagents into a favorable transition state structure. Among the possible approaches aiming to design the more efficient catalytic system, mass spectrometry, which detects ionic species, represents a valid support in the first stage of screening of reaction conditions (i.e. does the catalyst work? what is the best molar ratio of reagents? and the best solvent, acid additive), as well as in more specific experiments aimed at studying a peculiar aspect of the catalytic process (i.e. kinetic of reaction, detection of active intermediates or complexes, undesirable side reactions).[5] Different MS interfaces (ESI, APCI, DESI, MALDI DART, etc.) were employed to extend the power of technique where the concept of "soft" ionization became prominent to accept the equivalence between the ions and ionizable species existing in solution with those in gas phase.[6] Because ESI is especially suitable for the detection of small to medium molecular-weight molecules (common mass range *m/z* 100–2000) and it is also available in less specialized analytic MS laboratories, ESI-MS is very useful in studies of organic reactions. When designed to understanding the mechanism of catalytic cycles, ESI-MS and MS^n experiments were supported by computational data[7] and represent an alternative to other techniques (NMR, UV etc).[8] Reaction monitoring occurs in-continuous (on-line) or point-by-point (off-line) modes, depending mainly on the rate of the studied reactions. Fast reactions, air sensitive, and short-lived reaction intermediates require necessary on-line experiments. Off-line reaction monitoring is suitable for the kinetic study of slow reactions (more than several tens of minutes) and long-lived reaction intermediates (lifetime >1 min). Unfortunately, in the context of asym-

[a] *A. Iazzetti*
Department of Basic Biotechnological Sciences, Intensivological and perioperative clinics, Catholic University of Sacred Heart
L. go F. Vito 1, 00168 Rome, Italy
[b] *G. Mazzoccanti, A. Calcaterra, Prof. C. Villani, Prof. A. Ciogli*
Department of Chemistry and Drug Technology, Sapienza University of Rome
Piazzale A. Moro 5, 00185 Rome, Italy
E-mail: alessia.ciogli@uniroma1.it
https://phd.uniroma1.it/web/Alessia-Ciogli_nC2150_IT.aspx
[c] *Prof. G. Bencivenni, Prof. P. Righi*
Department of Industrial Chemistry "Toso Montanari", University of Bologna
Viale del Risorgimento 4, 40136 Bologna, Italy

Supporting information for this article is available on the WWW under https://doi.org/10.1002/ejoc.202101272

Part of the "Organocatalysis" Special Collection.

Research Article
doi.org/10.1002/ejoc.202101272

metric reactions, the main limitation of the ESI-MS lies in not giving, in a direct way, information on the stereoselectivity of the reaction. In fact, mass spectrometry has been considered a "chiral-blind" technique, not able to differentiate two enantiomers.[9] Challenging papers have reported the use of ESI-MS back-reaction screening of mass-labelled quasi-enantiomeric substrates (products) to provide the enantioselectivity of catalytic reactions.[10] However, this approach is time-consuming in the screening of reaction conditions and scope stages. Currently, enantioselective HPLC, by using a wide applicability chiral stationary phase (e.g., amylose- and cellulose-based), remains the most used technique to monitor the stereoselectivity of asymmetric reactions.

Here we report the off-line ESI-MS reaction monitoring experiments applied in catalytic processes mediate by well-known chiral primary amines (Figure 1). The work aims to demonstrate the utility of this approach for an alternative screening of reaction conditions, a better understanding of reaction mechanism and for obtaining preliminary results about reaction rate.

Results and Discussion

Analyzing published papers, metalloorganic mediated processes and organocatalytic reactions have benefited on the use of mass spectrometry to gain insights into the mode of catalyst activation.[11] Focusing to the aminocatalysis, the catalysts, their intermediates (enamine or iminium ion), the active catalyst-substrate complexes (via noncovalent bonding) and products are easy ionizable and then suitable candidates to be explored by ESI-MS approach. In addition, the detection of ion signal intensities over the time provides information both on reaction mechanism and how fast the reaction is. To confirm this, we started the investigation of the Friedel–Crafts alkylation of 2-methylindole and (E)-3-octen-2-one promoted by 9-amino(9-deoxy)epi-quinine (catalyst **1**) in toluene (Scheme 1, **i**) as prototypical reaction. The mechanism of reaction was deeper investigated by computational analysis and supported by experimental data.[12]

In our case, the reaction was conducted at room temperature for 24 hours with the only scope to detect relevant ions. By infusion the reaction mixture in positive mode ESI source, all species engaged in the mechanism have been easily detected. Figure 2 shows all species involved in the mechanism as reported in[12] but in the positively charged state together with the full scan spectrum after 24 hours of reaction. Briefly, the α-β-unsaturated ketone is activated by catalyst **1** through the iminium ion formation followed by addition of 2-methylindole and formation of intermediate **III**. Its hydrolysis provides the product **IV**. By flow injection analysis of diluted reaction mixture and working in ESI positive mode, the mass spectrum presents some signals in agreement with expected species: catalyst **1** (**I**, *m/z* 324.42), the iminium ion (**II**, *m/z* 390.33) and the iminium ion of product (**III**, *m/z* 521.42). This signal appears in a

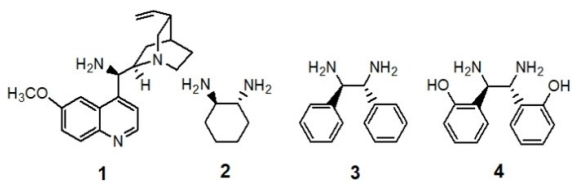

Figure 1. Chiral catalysts employed in this work.

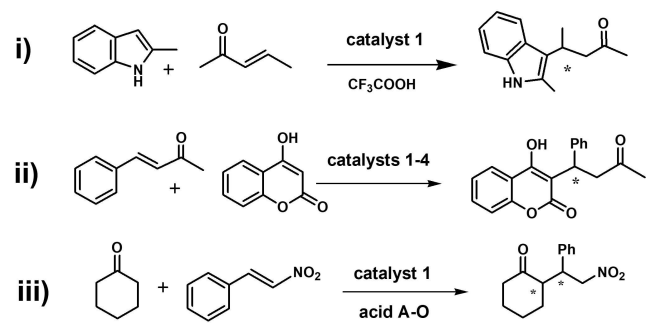

Scheme 1. Reaction investigated by ESI-MS.

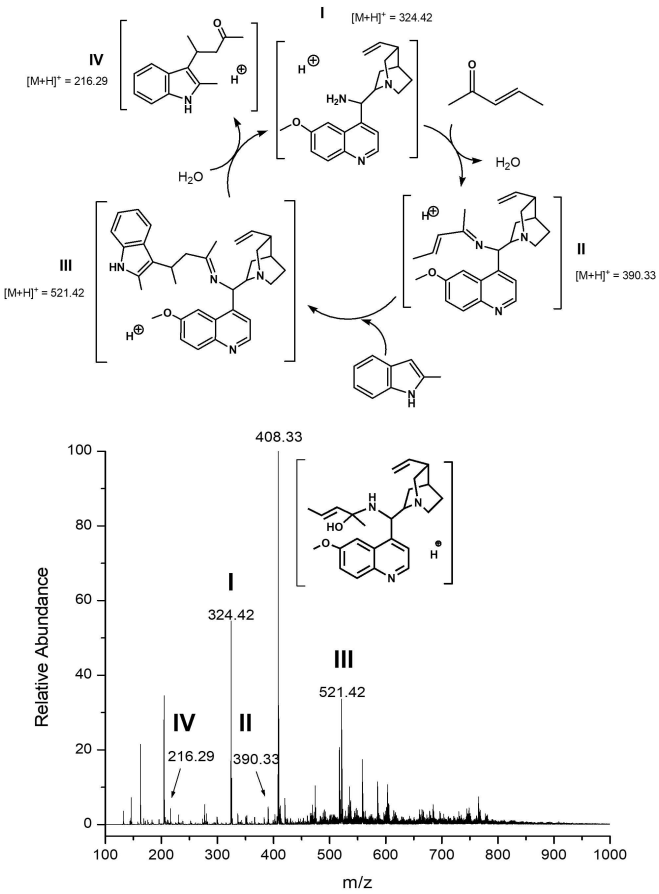

Figure 2. Top: All species involved in reaction represented as positively charged. Bottom: ESI-MS spectrum of reaction mixture at 24 h of starting. Recorded ions and their correlation with intermediates, catalyst and product were matched in the full spectrum. (Protonation sites are not specified in all reported structures).

permanent manner after 2.5 hours from the beginning of reaction.

It is also remarkable the presence of the hemiaminal (*m/z* 408.33). The signal of product (**IV**, *m/z* 216.29) was always detectable but with low intensity. The correlation between the structures of reaction intermediates and recorded ions has been supported by collision induced dissociation (CID) experiments. Fragments of *m/z* 408.33 validate the nature of carbinolamine: *m/z* 324.25 refers to the aminocatalyst and *m/z* 390.33 to the imine (loss of water, see Supporting Info, pag. 6). The presence of adducts with trifluoroacetic acid are not detected and therefore not showed in the catalytic cycle although the acid plays an important role in the stereocontrol of reaction.[12] Similar partners, via iminium ion cycle, have been correlated with the ions recorded by infusion of diluted mixture of reactants to prepare warfarin (Scheme 1, **ii**). The putative catalytic cycle was in Supporting Info at pag. 20. The reaction has been studied for 12 hours acquiring both positive and negative spectra. The acquisition in ESI negative mode was selected to confirm and to control the presence of product (*m/z* 307.08) since it preferentially undergoes negative ionization[13] (Supporting Info pages 14–15).

The value has been also validated by high-resolution-MS experiments (*m/z* 307.0976, $\Delta m = 0.198$ ppm). Switching the acquisition in positive mode, interesting results on the active reaction intermediates have been found. As reported in Figure 3, after 1.5 h from beginning, the main signal present in the spectrum is *m/z* 614.42 (Figure 3B). Zooming the *m/z* 50–500 region, significant ions were present (Figure 3A). The intense signals correspond to *m/z* 324.33 ion (the catalyst), the *m/z* 307.75 ion (typical partner of catalyst **1**) and the *m/z* 452.33 ion (the iminium ion). Less detectable ions were *m/z* 331.17 (product as sodium adduct) together with the *m/z* 470.42 signal of hemiaminal. The analysis of *m/z* 614.42 ion does not provide an exhaustive interpretation. As reported in Figure 3, two possible structures match with this signal: the covalent adduct of 4-hydroxycoumarin and the iminium ion intermediate or the analog non-covalent adduct. The CID MS^2 suggests that the ion loses a fragment corresponding to *m/z* 162 producing *m/z* 452.42 (Figure 3C), however it does not clarify the covalent or non-covalent nature of the intermediate. Considering that the CID spectrum has been recorded at the beginning of reaction (after 10 min of reaction start), it is plausible to assume that in the initial stage there is a non-covalent adduct between the two parts which later becomes of covalent nature. Looking in negative mode, the *m/z* 614.42 ion corresponds to *m/z* 612.42 one and its intensity trend, over the time, changes in opposite mode respect to the *m/z* 307.08 signal of reaction product, in line with the proposed catalytic process. All CID and HR-MS spectra of significant species useful, to confirm the nature of ions, are gathered in Supporting Info. To extend the ESI-MS approach also to the other aminocatalysts, we investigated the same reaction catalyzed by chiral vicinal aliphatic diamines **2**–**4**. Chin explored the reaction using catalysts **2** and **3**[15] while we introduced catalyst **4** inspired by the work of Zlotin.[16] In a typical experiment, small amount of ongoing reaction was largely diluted in methanol and introduced by infusion into ESI source to collect spectra producing a series of time points. The reaction mixtures were stirred in THF at room temperature with (10-fold excess) or without acetic acid. In all spectra, signals corresponding to monoimine protonated intermediate between benzylideneacetone and each catalyst were found. Spectra in Figure 4 were selected from the spectra collection reported in Supporting Information (pages 21–58) and show the ions of reaction mixtures mediate by catalyst **3** and catalyst **4** respectively. At reaction times of 30 min and 40 min, ions *m/z*

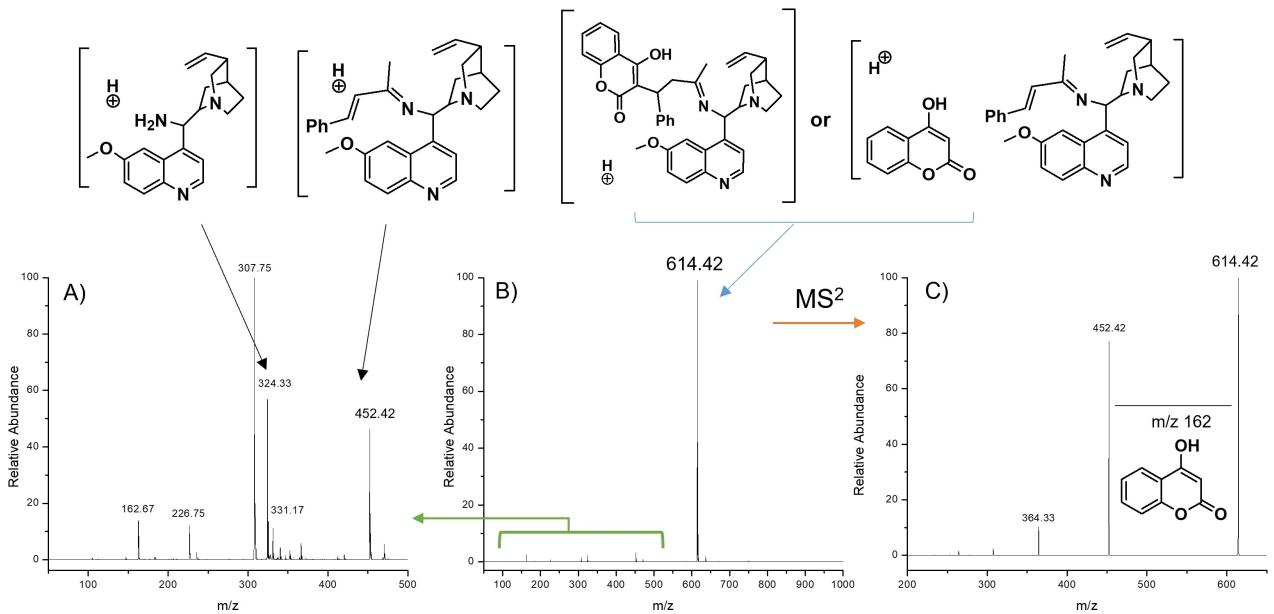

Figure 3. ESI-MS spectra of reaction **ii)** mixture at 1.5 h of starting. Full spectrum in *m/z* 50–500 range (A) and *m/z* 50–1000 range (B). MS^2 spectrum (C) of parent *m/z* 614 after 10 min of reaction start.

Research Article
doi.org/10.1002/ejoc.202101272

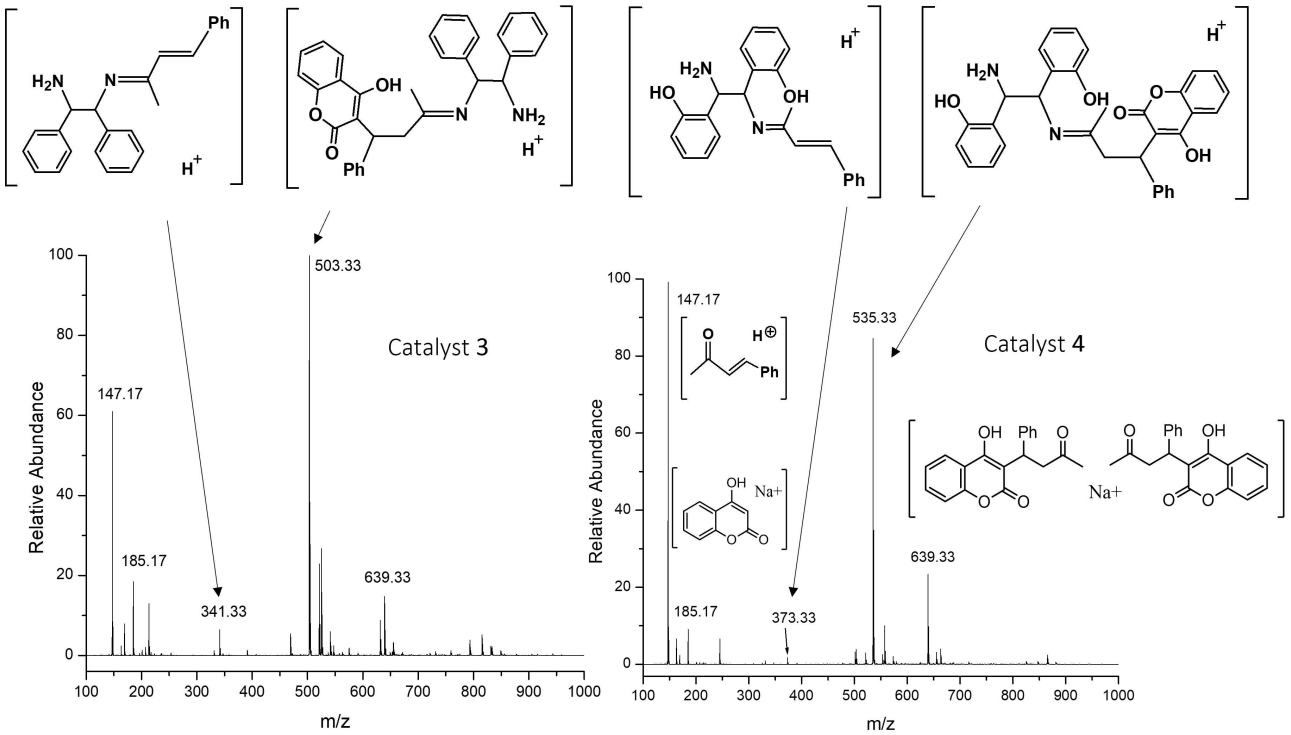

Figure 4. Full mass spectrum in ESI (+) of reaction mixture mediated by catalyst **3** and catalyst **4** without the acetic acid as cocatalyst. Samples were infused after methanolic dilution. The plausible adduct for *m/z* 535.33 and *m/z* 503.33 was describe as covalent adduct.[14]

503.33 and *m/z* 535.33 were more intense respect to the signal of product recorded as non-covalent dimer *m/z* 639.33 $[2\,M+Na]^+$. At the same reaction time, the ion of product dominates the spectrum when catalyst **2** was employed (Supporting Info page 21). This is due to reaction rate which in this case is higher and leads to completion in 24 h. These data agree with those proposed by Herrera et. al. and exclude the presence of a diimine intermediate which involve both amino groups as reported by Chen. By complete inspection of spectra, two signals corresponding to reagents were also found: *m/z* 147.17 and *m/z* 185.17 ions in agreement with the benzylideneacetone $[M+H]^+$ and the 4-hydrocoumarin $[M+Na]^+$ respectively. Focusing the attention to *m/z* 405.25, *m/z* 503.33 and *m/z* 535.33 ions (each ion for each employed catalyst) we observed a decrease of their relative abundance over the time as the intensity of product ions increases. Additional CID experiments attest their involvement in the catalytic cycle producing ions that can be associated with reagents or intermediates present on reactions (CID 10%, 15% and 20% as arbitrary unit; spectra in Supporting info pages 30, 36, 57). Similarly, to what was seen above, it was not possible to understand the nature, covalent or non-covalent, of the intermediates. A typical pathway fragmentation has been reported in Figure 5. When catalyst **2** was employed, parent ion of *m/z* 405.33 was recorded and its MS^2 fragmentation furnish the *m/z* 243.25. In figure, plausible structures of involved intermediates are also depicted.

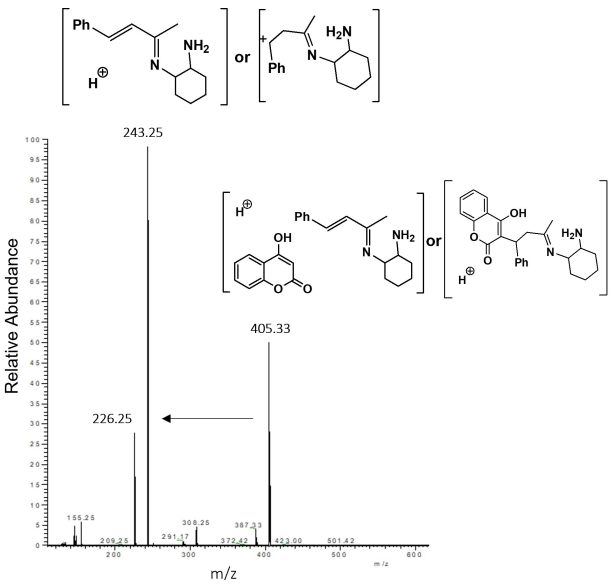

Figure 5. CID of isolated *m/z* 405.33 for reaction mediated by catalyst **2** at 10% of collision energy: main generated fragment was *m/z* 243.25. Plausible structures relating parent and daughter signals were reported.

If the acquisition in ESI (+) helps in the record of active intermediates and catalysts, the analysis of ESI (−) spectra allow some qualitative indications on the catalytic ability of employed diamines. In this case the intensities of negative ion referring to the product (*m/z* 307.08) were plotted against the reaction time together with the intensities of *m/z* 161.08 (4-hydroxycoumarin). The values relate to the catalytic reactions in absence of the acid co-catalyst. As visible in Figure 6, catalysts **3** and **4** show a comparable production speed (similar slope), while 1,2-dia-

Research Article
doi.org/10.1002/ejoc.202101272

Chemistry Europe
European Chemical Societies Publishing

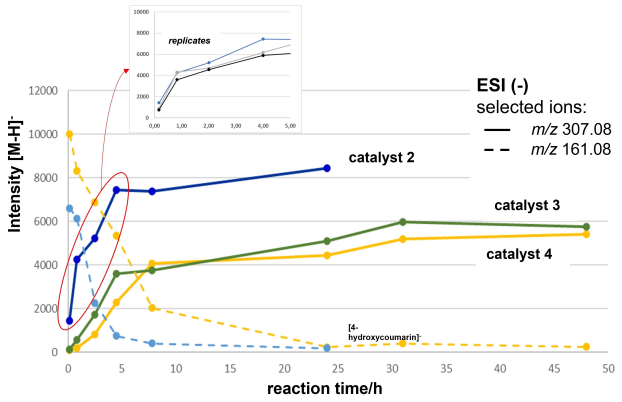

Figure 6. Intensity of ion referring to product (warfarin, *m/z* 307.08) vs reaction time. Dotted lines refer to the intensity of 4-hydroxycoumarin (*m/z* 161.08). Lines stopped at 24 h refer to the reactions catalyzed by diamine-cyclohexane. All data are reported without any correction.

mine-cyclohexane (catalyst **2**) catalyzes reaction faster. Moreover, the consuming of 4-hydroxycoumarin (dotted lines in Figure 6) nicely agrees with the corresponding increase of product. In addition, the insert in figure shows the values of 3 replicate experiments for reaction mediated by catalyst **2** in the first 4 h of reaction progress. Data are reported without any correction and therefore no indications on yield can be extrapolated which in any case has settled high values (>90%). Looking to the stereoselectivity, the enantioselective HPLC of crude reaction provide information on preferred enantiomer production. As reported in Table 1, while catalyst **2** shows poor stereocontrol of reaction regardless of the presence of the acid, catalyst **3** meaningfully benefits to the acetic acid in the mixture (enantiomeric ratio 92/8 vs 86/14). This agrees with an acid-base reaction between the second amino group and one equivalent of acid [1.l] providing a three-component catalytic cycle with one protonated amino group and the second involved in the iminium intermediate. Interesting, catalyst **4** allows good stereocontrol of the reaction which remains unaffected if in the presence of the acid (entries 5 and 6 in Table 1). This result suggests the formation of properly located hydrogen bonding between the hydroxyl group and one of both amino groups making a more rigid structure of the intermediate which improve an internal stereocontrol.

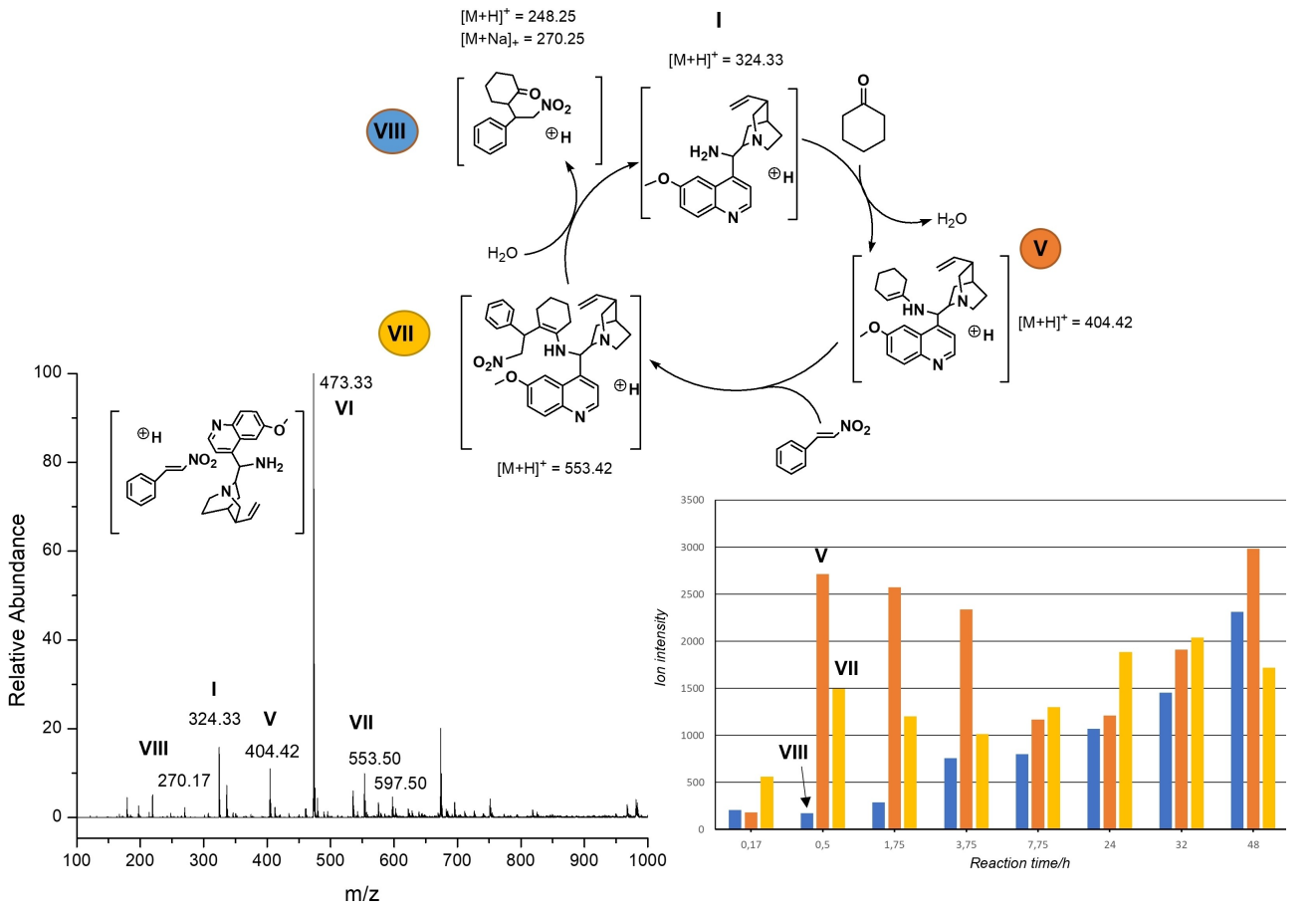

Figure 7. Top: Plausible catalytic cycle of reaction. All involved species are as positively charged. Structure **V** has been reported as protonated enamine instead of two possibility enamine/iminium ion to simply the scheme. Bottom left: Full mass spectrum at 1 h of reaction: all charged species of catalytic process (**VIII**, **V**, **VI**, **VII**) and a hypothetical by-product sample (*m/z* 597.50) have been recorded. Signal at *m/z* 673 has not been assigned. Bottom right: Plot reports the trend of **V**, **VII**, **VIII** ion intensities over 48 h. For data interpretation see in the text.

Table 1. Stereoselectivity of reaction in presence or without acid co-catalyst.

Entry	Catalyst[a]	Acid[b]	Time	Enantiomeric ratio[c]
1	(*R*,*R*)-**2**	0	24	78/22
2	(*R*,*R*)-**2**	10	24	76/24
3	(*R*,*R*)-**3**	0	48	86/14
4	(*R*,*R*)-**3**	10	48	92/8
5	(*R*,*R*)-**4**	0	48	84/16
6	(*R*,*R*)-**4**	10	48	88/12

[a] 10% mol of hydroxycoumarin. [b] 10-fold mol. [c] on Chiralpalk IB (Chromatograms are in Supporting Info).

In the second part of work, we investigated a Michael addition of cyclohexanone to β-trans-nitrostyrene (reaction **iii** in Scheme 1), a widely known reaction in the activation of cyclic saturated ketones which introduces two stereogenic centers with high stereocontrol when catalyst **1** is employed.[17] To the best of our knowledge, this reaction has never been investigated by ESI-MS. We started by studying the progress of the reaction in optimal working condition (toluene as solvent, benzoic acid as cocatalyst, 48 h).

The hypothetical catalytic cycle starts with the activation of cyclohexanone by the catalyst **1** forming the iminium ion/enamine intermediate (structure **V** in Figure 7). The activation of cyclohexanone is promoted by an acid cocatalyst, the benzoic acid in the model reaction. Unfortunately, mass spectrometry cannot discriminate between the active protonated enamine or iminium ion isomers as main form, being them isobaric.[18] From now, to simplify the reader in the lecture of schemes and figures, we select the protonated enamine as the active specie. The β-nitrostyrene then reacts with intermediate **V** to allow structure **VII** (drawn even in protonated enamine form). Hydrolysis of **VII** gave the product **VIII** closing the cycle. By offline reaction monitoring, the full mass spectra showed four ions reflecting all species present in the catalytic cycle: product (**VIII**), catalyst (**I**), and active intermediate of product (**VII**). In addition to these signals, the *m/z* 473.33 ion consistent with the non-covalent adduct between catalyst and β-nitrostyrene (**VI**) was also recorded. Figure 7 provide a picture of reaction mixture after 1 h. The ion at *m/z* 597.50, that constantly increases over reaction time, can be attributed to the oligomer of nitrostyrene (4 units) present as undesirable product due to a collateral catalytic polymerization reaction.[19] Additional CID experiments support the correlation between signal and structures (Supporting Info, pages 66–71). By analyzing how each ion intensity changes over reaction time, we observed i) the progressive grow of product signal **VIII**, ii) a fast production of **V** during the first 2 h, iii) the continued presence of ion **VII** (plot in Figure 7). The intensity of *m/z* 473.33 signal decreases over time (see Supporting Info pag. 71) The significant increase in the m/z 404.42 ion at the end of the reaction (reproducible trend in the various tested reaction) could be explained by the formation of the intermediate **V** with the ketone, in large excess on reaction, while the nitrostyrene is no longer available. After identification of charged species involved in the plausible catalytic cycle, we evaluated the effect of different acids as cocatalysts (A–N in Scheme 2) in i) the enamine/iminium ion formation, ii) the product formation and iii) the stereoselective ability. The first two aspect were investigated by mass spectrometry, the last by enantioselective HPLC directly on the crude reaction mixture. From the point of view of a purely qualitative screening, the most important variable to take into account in the treatment of the data obtained is the response of the ESI source in terms of spray reproducibility. Herein, to reduce the instrumental error, we used a solution of reserpine as an external standard. The values of the intensities of the studied ions (*m/z* 404.42 and *m/z* 270.17) were normalized for the value of the standard recorded before of each reaction withdrawal and the following data were reported in the plots in Figure 8. In terms of reaction progress, 10 min after addition of the acid, the enamine was mainly produced by *p*-methoxy and *p*-hydroxy benzoic acids (Figure 8, plot A), while the higher value of product ion was obtained by using *p*-nitro benzoic acid followed by 3,5-dinitro benzoic acid (Figure 8, plot B).[20] From the stereochemical point of view, high values of enantiomeric ratio were recorded in all cases but no one acid results prevalent.[21] Overall, balancing yield, d.r. (diastereomeric ratio) and e.r. (enantiomeric ratio) of the reaction, the 4-nitro benzoic acid seems to be the favorite partner as attested in the analogous reaction which involve β-trans-nitrostyrene.[22]

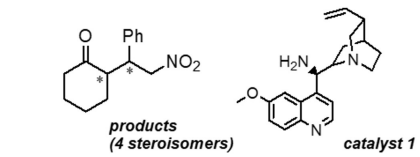

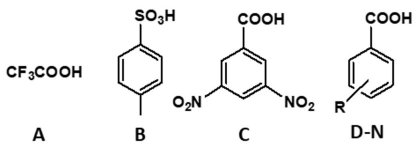

Acid	Substituent	pka/σ	d.r.	e.r.
C	3,5-DNB	2,81	86/14	89/11
D	R = 4-NO_2	3,44/0,78	90/10	89/11
E	R = 4-CF_3	3,69/0,54	85/15	85/15
F	R = 4-Br	3,96/0,232	82/18	88,5/11,5
G	R = 4-I	4,0/0,18	90/10	90,5/9,5
H	R = 4-F	4,14/0,062	90/10	91/9
I	R = H	4,20/0	87/13	91,5/8,5
L	R = 4-OCH_3	4,44/-0,268	85/15	91/9
M	R = 4-OH	4,54/-0,37	83/17	90/10
N	R = 2- NO_2	2,18	90/10	90,5/9,5

Scheme 2. Screening of investigated acid cocatalysts. Diastereomeric (d.r.) and enantiomeric (e.r.) ratios were determined by HPLC.[23]

Research Article
doi.org/10.1002/ejoc.202101272

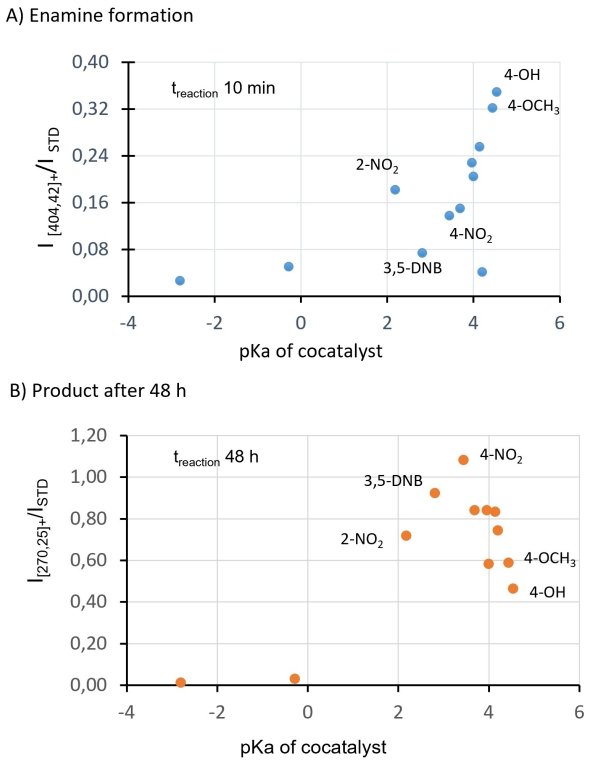

Figure 8. Signal referring to protonated enamine ion (**A**) and product ion (**B**) vs pKa of investigated acids, after 10 minutes and 48 h after the acid addition. Intensity values were normalized with the intensity of external standard recorded before the analysis of each sample.

Conclusion

In this work prototypical reactions catalyzed by the most popular primary amines and diamines (1,2-diaminocyclohexane, 1,2-diphenylethylenediamine, 9-amino-9-deoxy-9-epiquinine) were studied by mass spectrometry. The offline ESI-MS reaction monitoring provides a picture of reagents and products present with the relevant active intermediates that support the plausible catalytic cycle. Our experimental data show that this approach combined with enantioselective HPLC analysis could be useful in the screening of different organo-catalysts or in the selection of suitable cocatalyst. The methodology may have relevance to other reactivity work where iminium or enamine intermediates are involved, and it helps in the elucidation of the intrinsic properties of catalyst/co-catalyst pair that controls the reaction mechanism.

Experimental Section

Materials. The 9-amino-9-deoxy-9-epiquinine (catalyst **1**) was obtained as reported in.[24] Starting materials, acids A–O, solvents, as well as (1R,2R)-diaminocyclohexane (catalyst **2**), (1R,2R)-1,2-diphenylethylenediamine (catalyst **3**) and (1R,2R)-1,2-bis (2-hydroxyphenyl)ethylenediamine (catalyst **4**) are commercially available and were employed without further purification or treatment.

Mass Spectrometric Experiments. Studies were conducted on a Thermo Scientific (Bremen, Germany) LTQ mass spectrometer connected to a heated electrospray ionization (HESI) source. Compound samples were prepared by 1/10000 dilution in methanol or acetonitrile and were injected into the HESI source at a flow rate of 10 μL/min. The instrument was operated in positive ion mode with optimized HESI source conditions included needle potential of 4.2 kV, a heater temperature of 50 °C, a capillary temperature of 270 °C, capillary voltage 10 V, and tube lens voltages 50 V. Sheet gas flow rate was between 8–10 (arbitrary unit). Ions of interest for MS^n experiments were isolated with a *m/z* 3–5 window. The collision energy employed for collision induced dissociation (CID) spanned between 10 % and 20 % (arbitrary unit of helium flow). Data were collected using 30 scans and taking a mass range between m/z 100–1000. To control the constant response by time of ESI-MS, a standard methanolic solution of reserpine ([M + H] + m/z 609.33, 10^{-6} M, grade MS sample quality) with the tuned settings reported above was injected (and data was acquired) at the beginning of each data collection session. These data represent our external standard employed to compare ion intensity between different experiments.

All reactions were made in small vials under magnetic stirring. All reactants were in sequence (the acid at the end) added to solvent.

Catalytic Reaction A. 2-methylindole (C_9H_9N, Mw 131.17, 0.13 mmol, 17 mg), (E)-3-octen-2-one (C_5H_8O, Mw: 84.12, 0.10 mmol, 0.01 mL), catalyst **1** ($C_{20}H_{25}N_3O$, M_w: 323.43, 0.019 mmol) and trifluoroacetic acid ($C_2HF_3O_2$, Mw: 114.02, 0.039 mmol) were dissolved in toluene (500 ul) at room temperature with magnetic stirring. Reaction was monitored for 24 h.

Catalytic Reaction B. *For catalyst 1.* 4-hydroxycoumarin ($C_9H_6O_3$, Mw 162.14, 0.044 mmol, 7.2 mg), benzylideneacetone ($C_{10}H_{10}O$, Mw 146.19, 0.065 mmol, 9.5 mg), catalyst **1** (0.012 mmol) and trifluoroacetic acid ($C_2HF_3O_2$, Mw: 114.02, 0.026 mmol) were dissolved in dichloromethane (500 ul) at room temperature with magnetic stirring. *For catalyst 2–4.* 4-hydroxycoumarin ($C_9H_6O_3$, Mw 162.14, 0.12 mmol, 20 mg), benzylideneacetone ($C_{10}H_{10}O$, Mw 146.19, 0.15 mmol, 22 mg), catalyst **2**–**4** (0.012 mmol) and acetic acid ($C_2H_4O_2$, Mw: 60.00, mmol) were dissolved in THF (200 ul) at room temperature with magnetic stirring. Reaction with catalyst **1** was monitored for 12 h, while reactions with catalyst **2** for 24 h and catalysts **3**–**4** for 48 h respectively. In addition to the positive ESI-MS acquisitions, spectra in negative ion mode were recorded.

Catalytic Reaction C. Cyclohexanone ($C_6H_{10}O$, M_w: 98.15, 0.96 mmol,100 μl), trans-β-nitrostyrene ($C_8H_7NO_2$, M_w: 149.15, 0.15 mmol, 22 mg), acid co-catalyst **A**–**O** (0.055 mmol) were dissolved in toluene (100 μl) at room temperature with magnetic stirring. The 9-amino-9-deoxy-9-epiquinine (catalyst **1**, $C_{20}H_{25}N_3O$, M_w: 323.43, 0.05–0.04 mmol, 17–13 mg) was lastly added corresponding to the start of reaction. Off-line reaction monitoring was done collecting samples after 10 min (t_1), 30 min (t_2), 1 h 45 min (t_3), 3 h 45 min (t_4),7 h (t_5), 21 h (t_6), 24 h (t_7) and 48 h (t_8).

All spectra, MS signal intensity tables, inter- and intraday response of HESI-MS and HPLC traces to determine the reaction stereoselectivity were in Supporting Information.

Acknowledgement

The study was supported by Ateneo 2020 founds from Sapienza University of Rome. Open Access Funding provided by $INSTITUTION within the CRUI-CARE Agreement.

Conflict of Interest

The authors declare no conflict of interest.

Keywords: Aminocatalysis · Mass spectrometry · Michael addition · Reaction monitoring · Reaction mechanism

[1] a) B. List, *Chem. Commun.* **2006**, *8*, 819–824; b) M. Nielsen, D. Worgull, T. Zweifel, B. Gschwend, S. Bertelsena, K. A. Jørgensen, *Chem. Commun.* **2011**,*47*, 632–649; c) J. Dai, Z. Wang, Y. Deng, L. Zhu, F. Peng, Y. Lan, Z. Shao, *Nat. Commun.* **2019**, *10*, 5182; d) W. Notz, F. Tanaka, C. F. Barbas, *Acc. Chem. Res.* **2004**, *37*, 580–591; e) G. Lelais, D. W. C. MacMillan, *Aldrichimica Acta* **2006**, *39*, 79–87; f) S. Mukherjee, J. W. Yang, S. Hoffmann, B. List *Chem. Rev.* **2007**, *107*, 5471–5569; g) A. Erkkilä, I. Majander, P. M. Pihko *Chem. Rev.* **2007**, *107*, 5416–5470; h) P. Melchiorre, M. Marigo, A. Carlone, G. Bartoli, *Angew. Chem. Int. Ed.* **2008**, *47*, 6138–6171; *Angew. Chem.* **2008**, *120*, 6232–6265; i) P. Melchiorre, *Angew. Chem. Int. Ed.* **2012**, *51*, 9748–977; *Angew. Chem.* **2012**, *124*, 9886–9909; j) I. G. Sonsona, E. Marqués-Lòpez, M. Concepciòn Gimeno, R. P. Herrera, *New J. Chem.* **2019**, *43*, 12233–12240; k) P. Vízcaíno-Milla, J. M. Sansano, C. Nájera, B. Fiser, E. Gómez-Bengo, *Synthesis* **2015**, *47*, 2199–2206; l) Ł. Wozniak, G. Magagnano, P. Melchiorre, *Angew. Chem. Int. Ed.* **2018**, *57*,1068–1072; *Angew. Chem.* **2018**, *130*, 1080–1084.

[2] a) F. Peng, Z. Shao, *J. of Molecular Catalysis A: Chemical* **2008**, *285*, 1–13; b) L.-W. Xu, J. Luo, Y. Lu, *Chem. Commun.* **2009**, *14*, 1807–1821; c) L. Jiang, Y.-C. Chen, *Catal. Sci. Technol.* **2011**, *1*, 354–365; d) J. Dai, D. Xiong, T. Yuan, J. Liu, T. Chen, Z. Shao, *Angew. Chem. Int. Ed.* **2017**, *56*, 12697–12701; *Angew. Chem.* **2017**, *129*, 12871–12875; e) G. Zhan, W. Du, Y.-C. Chen, *Chem. Soc. Rev.* **2017**, *46*, 1675–1692; f) L. Zhang, N. fu, S. Luo, *Acc. Chem. Res.* **2015**, *48*, 986–997; g) Y–H. Zhou, Y.-Z. Zhang, Z.-L. Wu, T. Cai, W. Wen, Q.-X. Guo, *Molecules* **2020**, *25*(3), 648.

[3] a) M. Amedjkouh, *Tetrahedron: Asymmetry* **2005**, *16*, 1411–1414; b) F. Tanaka, R. Thayumanavan, N. Mase, C. F. Barbas III, *Tetrahedron Lett.* **2004**, *45*, 325–328.

[4] a) S. Crotti, N. Di Iorio, C. Artusi, A. Mazzanti, P. Righi, G. Bencivenni, *Org. Lett.* **2019**, *21*, 9, 3013–3017; b) Y.-S. Huang, S.-G. Song, L. Ren, Y.-G. Li, X. Wu, *Eur. J. Org. Chem.* **2019**, *40*, 6838–6841; c) G. Bergonzini, S. Vera, P. Melchiorre, *Angew. Chem. Int. Ed.* **2010**, *49*, 9685–9688; *Angew. Chem.* **2010**, *122*, 9879–9882.

[5] a) C. Iacobucci, S. Reale, F. De Angelis, *Angew. Chem. Int. Ed.* **2016**, *55*, 2980–2993; *Angew. Chem.* **2016**, *128*, 3032–3045; b) D. Schröder, *Acc. Chem. Res.* **2012**, *45*, 1521–1532; c) G.-J. Cheng, X. Zhong, Y.-D. Wu, X. Zhang, *Chem. Commun.* **2019**, *55*, 12749–12764; d) W. Zhu, Y. Yuan, P. Zhou, L. Zeng, H. Wang, L. Tang, Bin Guo, B. Chen, *Molecules* **2012**, *17*, 11507–11537.

[6] a) A. Ray, T. Bristow, C. Whitmore, J. Mosely, *Mass Spectrom. Rev.* **2018**, *37*, 565–579; b) K. L. Vikse, J. S. McIndoe, *Pure Appl. Chem.* **2015**, *87*(4), 361–377; c) L. P. E. Yunker, R. L. Stoddard, J. S. McIndoe, *J. Mass Spectrom.* **2014**, *49*, 1–8:; d) L. S. Santos, *Eur. J. Org. Chem.* **2008**, 235–253; e) X. Ma, S. Zhang, X. Zhang, *TrAC Trends Anal. Chem.* **2012**, *35*, 50–66; f) K. Masuda, S. Kobayashi, *Chem. Sci.* **2020**, *11*, 5105–5112.

[7] a) J. A. Willms, R. Beel, M. L. Schmidt, C. Mundt, M. Engeser, *Beilstein J. Org. Chem.* **2014**, *10*, 2027–2037; b) M. W. Alachraf, R. C. Wende, S. M. M. Schuler, P. R. Schreiner, W. Schrader *Chem. Eur. J.* **2015**, *21*, 16203–16208; c) B.-L. Li, Y.-F. Wang, S.-P. Luo, A.-G. Zhong, Z.-B. Li, X.-H. Du, D.-Q. Xu, *Eur. J. Org. Chem.* **2010**, 656–662.

[8] a) R. Theron, Y. Wu, L. P. E. Yunker, A. V. Hesketh, I. Pernik, A. S. Weller, J. S. McIndoe, *ACS Catal.* **2016**, *6*, 6911–6917; b) K. M. Diemoz, J. E. Hein, S. O. Wilson, J. C. Fettinger, A. K. Franz, *J. Org. Chem.* **2017**, *82*, 6738–6747; c) K. M. Diemoz, A. K. Franz, *J. Org. Chem.* **2019**, *84*(3), 1126–1138; d) E. L. Myers, M. J. Palte, R. T. Raines, *J. Org. Chem.* **2019**, *84*(3), 1247–1256; e) T. Kumpulainen, J. Qian, A. M. Brouwer *ACS Omega* **2018**, *3*, 1871–1880.

[9] H. Awad, A. El-Aneed, *Mass Spectrom. Rev.* **2013**, *32*, 466–483.

[10] a) C. Markert, P. Rçsel, A. Pfaltz, *J. Am. Chem. Soc.* **2008**, *130*, 3234–3235; b) C. Ebner, C. A. Müller, C. Markert, A. Pfaltz *J. Am. Chem. Soc.* **2011**, *133*, 4710–4713; c) I. Fleischer, A. Pfaltz, *Chem. Eur. J.* **2010**, *16*, 95–99; d) F. Bächle, J. Duschmalé, C. Ebner, A. Pfaltz, H. Wennemers, *Angew. Chem. Int. Ed.* **2013**, *52*, 12619–12623; *Angew. Chem.* **2013**, *125*, 12851–12855.

[11] a) C. Vicent, D. G. Gusev, *ACS Catal.* **2016**, *6*, 3301–3309; b) P. Chen, *Angew. Chem. Int. Ed.* **2003**, *42*, 2832–2847; *Angew. Chem.* **2003**, *115*, 2938–2954; c) H. Wang, Y. Li, R. Zhang, K. Jin, D. Zhao, C. Duan, *J. Org. Chem.* **2012**, *77*, 4849–4853; d) C. Singh, M. K. Gangwar, P. Ghosh, *Inorg. Chim. Acta* **2017**, *466*, 358–369; e) K. L. Vikse, Z. Ahmadi, J. S. McIndoe, *Coord. Chem. Rev.* **2014**, *279*, 96–114; f) X. Yan, E. Sokol, X. Li, G. Li, S. Xu, R. G. Cooks, *Angew. Chem. Int. Ed.* **2014**, *53*, 5931–5935; *Angew. Chem.* **2014**, *126*, 6041–6045; g) A. Schnell, J. A. Willms, S. Nozinovic, M. Engeser, *Beilstein J. Org. Chem.* **2019**, *15*, 30–43; h) M. Cai, K. Xu, Y. Li, Z. Nie, L. Zhang, S. Luo, *Am. Chem.* **2021**, *143*, 1078–1087.

[12] A. Moran, A. Hamilton, C. Bo, P. Melchiorre, *J. Am. Chem. Soc.* **2013**, *135*, 9091–9098.

[13] C. I. Gioumouxouzis, M. G. Kouskoura, C. K. Markopoulou, *J. Chromatogr. B* **2015**, *998–999*, 97–105.

[14] Methanol and acetonitrile are routinely solvents used in FIA-MS experiments. To demonstrate that large dilution of crude of reaction do not change the TIC response, one rection has been studied over time using both solvents, as reported in Supporting Info (page 59). TIC spectra provide equivalent information in terms of ions and trend of ion intensities during reaction time. Slightly differences in relative intensities were observed due to different desolvation power of two solvents.

[15] H. Kim, C. Yen, P. Preston, J. Chin, *Org. Lett.* **2006**, *8*(23), 5239–5242.

[16] A. S. Kucherenko, A. A. Kostenko, G. M. Zhdankina, O. Yu. Kuznetsova, S. G. Zlotin, *Green Chem.* **2018**, *20*, 754–759.

[17] S. H. McCooney, S. J. Connon, *Org. Lett.* **2007**, *9*(4), 599–602.

[18] a) Y. Ren, O. Kravchenko, O. Ramström, *Chem. Eur. J.* **2020**, *26*, 15654–15663; b) X. Jie, Y. Shang, Z.-N. Chen, X. Zhang, W. Zhuang, W. Su, *Nat. Commun.* **2018**, *9*, 5002.

[19] M. E. Carter, J. L. Nash Jr, J. W. Drueke Jr, J. W. Schwietert, G. B. Butler *J. Polym. Sci. Polym. Chem. Ed.* **1978**, *16*, 937–959.

[20] Plots in Figure 8 furnish a qualitative point of view of reactions, nonquantitative data can be extract from them. In any case, yield was verified by product isolation (as enantiomer mixture) and both acids afford to 60–70% of product.

[21] Looking to the minor product, the p-Br and p-OH benzoic acids promote a slightly stereocontrol toward a single enantiomer, but the stereochemical preference is opposite (Supporting Info, page 72).

[22] a) D. Almas, D. A. Alonso, E. Gómez-Bengoa, Y. Nagel, C. Nájera, *Eur. J. Org. Chem.* **2007**, 2328–2343; *Angew. Chem. Int. Ed.* **2007**, *46*, 6915–6917; *Angew. Chem.* **2007**, *119*, 7040–7042; b) N. Kaplaneris, G. Koutoulogenis, M. Raftopoulou, C. G. Kokotos, *J. Org. Chem.* **2015**, *80*, 5464–5473; c) M. Tsakos, M. R. J. Elsegood, C. G. Kokotos, *Chem. Commun.* **2013**, *49*, 2219–2221.

[23] A. Ciogli, D. Capitani, N. Di Iorio, S. Crotti, G. Bencivenni, M. P. Donzello, C. Villani, *Eur. J. Org. Chem.* **2019**, *10*, 2020–2028.

[24] C. Cassani, R. Martin-Rapun, E. Arceo, F. Bravo, P. Melchiorre, *Nat. Protoc.* **2013**, *8*, 325–344.

Manuscript received: October 15, 2021
Revised manuscript received: November 1, 2021
Accepted manuscript online: November 6, 2021